DEVELOPMENT OF
MOBILE MACHINING CELL

Portable machine(s)

Workpiece

Global referencing system

Workshop floor

DATA SHEET

Titel: Development of Mobile Machining Cell
Subtitle: Mechanical Engineering
Series title and no.: Technical report ME-TR-10

Author: Kasper Ringgaard
Department of Engineering – Mechanical Engineering, Aarhus University

Abstract: This report covers some initial aspects of development of the mobile InnoMill machining cell. The new machining paradigm where the machine is mounted on the workpiece is compared to the old paradigm where the workpiece is mounted inside the machine, and differences are discussed. Parametric studies of the workpiece case study of the InnoMill project, the Vestas V112-3.0MW wind turbine hub, are performed to supply insight regarding load capacity etc. for the machine designers. The hub finite element model is validated using experimental results from Operational Modal Analysis performed on the hub. Furthermore, the InnoMill concept is described, and work regarding the 6 degree of freedom parallel kinematic manipulator which is present in the concept is performed. A numerical procedure accounting for base deflections due to static loading is proposed and implemented. Additionally, a six degree of freedom spring-mass model vibrational response is compared to vibrational response obtained from experiments on the 6 degree of freedom parallel kinematic manipulator at Aarhus University. The model, which is based on assumptions commonly found in literature, is rejected.
Finally, a outlook for the remaining part of the PhD project is presented and described.

Cover image: Kasper Ringgaard & CNC Onsite A/S

DEVELOPMENT OF MOBILE MACHINING CELL

Kasper Ringgaard, Aarhus University

Abstract

This report covers some initial aspects of development of the mobile InnoMill machining cell. The new machining paradigm where the machine is mounted on the workpiece is compared to the old paradigm where the workpiece is mounted inside the machine, and differences are discussed. Parametric studies of the workpiece case study of the InnoMill project, the Vestas V112-3.0MW wind turbine hub, are performed to supply insight regarding load capacity etc. for the machine designers. The hub finite element model is validated using experimental results from Operational Modal Analysis performed on the hub. Furthermore, the InnoMill concept is described, and work regarding the 6 degree of freedom parallel kinematic manipulator which is present in the concept is performed. A numerical procedure accounting for base deflections due to static loading is proposed and implemented. Additionally, a six degree of freedom spring-mass model vibrational response is compared to vibrational response obtained from experiments on the 6 degree of freedom parallel kinematic manipulator at Aarhus University. The model, which is based on assumptions commonly found in literature, is rejected. Finally, a outlook for the remaining part of the PhD project is presented and described.

Contents

Introduction

The wind turbine industry strive to lower the cost of energy for their products, to cope with an increasing demand for cheap sustainable energy. To increase the power output the wind turbine manufacturers have developed immense wind turbines, which pushes the limits of the production methods currently available. A vast variety of the turbine components are manufactured using malleable cast iron, machined to fit tolerance requirements afterwards. Dimensions of the largest items exceed 3x3x3 meters.

Conventionally sized CNC[1] milling machines are build to contain the entire workpiece, which causes the overall dimensions of the machines to be governed by the workpiece sizes [1]. The *"Workpiece in Machine"* paradigm has been scaled from conventionally sized machines to machining of modern large scale components, leading to heavy and large CNC machines with workspaces covering several cubic meters. Building such large CNC machines requires large and expensive foundations, careful structural design and specialised control designs [1]. Therefore, purchasing such large machinery is a large investment, which eventually makes wind turbines more expensive.

1.1 InnoMill Project

To lower the cost of machining of large wind turbine components, a consortium of Danish industrial companies and universities has joined in the Innovation Fund supported InnoMill project. The basic idea of the project is to invert the old paradigm, leading to the paradigm being *"Machine on workpiece"* instead of *"Workpiece in Machine"*.

The goal is to build a mobile and reconfigurable machining cell, which can be relocated relative to the workpiece to reach the entire item being machined. Thus the size of the machine becomes independent of the workpiece size, thereby avoiding the need for large and heavy foundations and rigid and heavy machine parts. Eventually this leads to lower cost of the machine, which ensures cheaper production of wind turbines. The trade-off for the mobile machine is expected to be lower rigidity, leading to less productivity and accuracy than the CNC machines being used currently.

The aim of this work is to identify the problems arising with the new type of machining cell, and to develop remedies to the challenges regarding productivity and accuracy.

The wind turbine component studied in this project is the Vestas V112-3.0 MW hub. The partners participating in the project are Danish Technical University, Danish Advanced Manufacturing Research Center, Global Castings A/S, CNC Onsite A/S and Aarhus University, see Figure 1.1.

Figure 1.1: InnoMill Project Partners

---

[1]Computer Numerical Control

Problem Analysis

2.1 Machining

To ensure competitive product prices the cost of production has to be as small as possible. For machining high Material Removal Rate (MRR) is key when pursuing low production cost. The maximum MRR possible is constrained by the tolerance- and surface roughness requirements which manufacturers has to comply with. High MRR can be achieved by high feed rates and deep cuts. High feed rates yield large accelerations, which combined with large masses of the machine tool causes large inertia forces. Furthermore cutting forces are proportional to feed rate and depth of cut, which means that high MRR causes large cutting forces. In general, low forces and slow motion increases the accuracy obtainable with a machine tool and therefore high MRR and high accuracy counteract each other. Therefore, finding the optimal combination of machine tool and process parameters is a trade-off between efficiency and accuracy. In many cases this is based on a trial-and-error approach and experience of the machinist.

In recent years different research groups around the world have worked on developing methods for improving productivity and accuracy of machining processes.

One of the main limitations of increasing productivity in machining is a self-excited vibration phenomena called chatter [2]. Chatter can ruin the surface quality of the workpiece and damage the machine or cutting tool. New tool designs, better fixtures and active damping systems are proposed for improving the chatter stability of different machining setups. Furthermore experimental analysis and mathematical models of machine, tool and workpiece [3] are utilised for prediction of stability boundaries to allow optimization of the process parameters.

Another limitation is driven by tolerance requirements, which are challenged by deflections of workpiece, machine and cutting tool. Utilising detailed cutting force prediction models, finite element models of the workpiece and mathematical models of machine tools [4] cutting forces can be predicted and compensated for during toolpath planning. This enable deeper cuts without exceeding tolerance requirements. Furthermore, once the models are obtained they can be utilised for compensating deflections caused by other loads such as gravitational, thermal and clamping loads. Additionally the accuracy of the machining process also depends on the re-positioning accuracy of the machine tool [5], which depends on how accurately the machine is build. If large inaccuracies are present different measurements techniques can be utilised for mapping position error over the workspace [6]. The error maps are utilised for compensation of toolpath.

2.2 Comparison of Paradigms

Workpiece in Machine

Current machine tools for large wind turbine components are build following the paradigm *"Workpiece in Machine"*. The size of the Vestas V112-3.0 MW hub being more than 3x3x3 meters, leads to immense machine tools. Building such large machine tools is expensive and yields multiple challenges regarding accuracy and stability [1]. Figure 2.1a illustrates the basic topology of the machine tools used for machining the Vestas V112-3.0 MW hub by Global Castings A/S. The machine tool and the workpiece fixture are mounted on a heavy and rigid concrete foundation. The machine tool holds a high power spindle, which requires rigid machine and fixture structures to limit deflections. The global referencing system is well defined due

to the rigidity of the structure, and all motion of the tool tip is described using the machine axis encoders. The system exerts loads from the fixture clamping and cutting loads on the workpiece. The machine tool maximum feed rates are limited due to the large masses that needs to be moved. The machine is not scalable, since larger workpiece requires larger machine. The machine tool is used for all machining operations conducted (milling, drilling, tapping), hence it has an excess of power for the low power operations such as tapping.

Machine on Workpiece

The InnoMill machine is designed following the paradigm *"Machine on Workpiece"*. Figure 2.1b illustrates the basic idea of the InnoMill machine. The workpiece is placed on the workshop floor, and the mobile and reconfigurable machining cell is attached to the workpiece. The machine tool machines the reachable region, and is then relocated to the next position. The machine is relocated as many times as required to machine all features of the workpiece. This procedure makes the system scalable for all future sizes of components without having to build new machines. An external global referencing system is required to keep track of machine-to-workpiece relative position and orientation. Such external referencing capability can be realised using three dimensional metrology systems e.g. lasertrackers or computer vision [1, 7]. The workpiece is subjected to both cutting loads and the mass of the machine tool, which makes low weight of the machine tool important. Low weight can be achieved by choosing a small spindle and loosening stiffness requirements for the machine tool. Lower stiffness of the structure means that forces must be smaller to comply with tolerance requirements. Forces are lowered by limiting the MRR, but this might cause the new machining cell to be too inefficient. To maintain high MRR multiple machining cells can work in parallel. Furthermore developing special purpose units for milling, drilling and tapping respectively, it will be possible to maximize the efficiency of each subprocess.
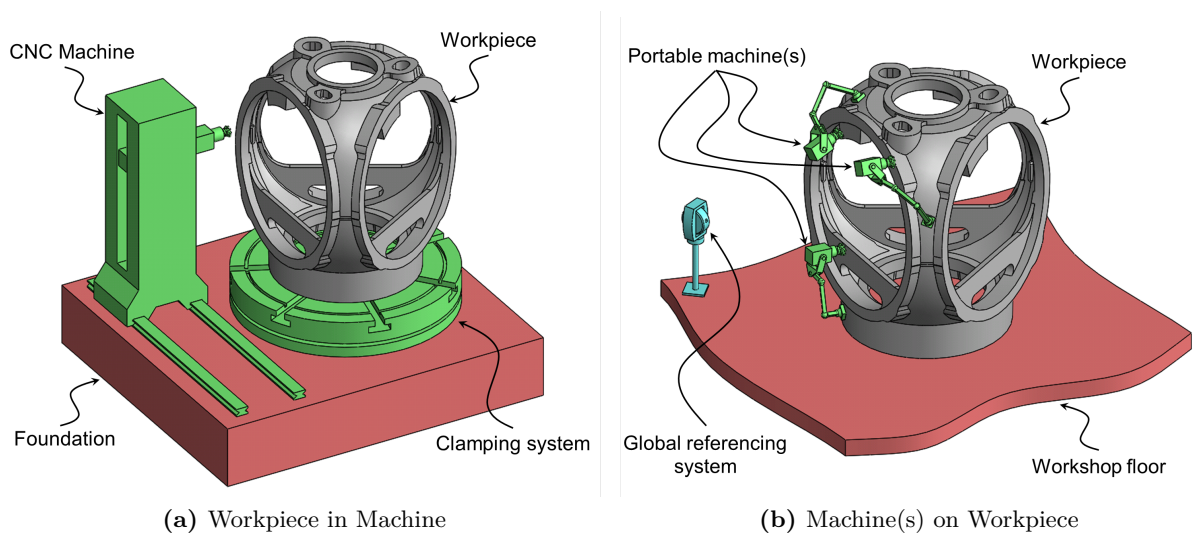

(a) Workpiece in Machine   **(b)** Machine(s) on Workpiece

Figure 2.1: Paradigms

Differences

The main differences between the two paradigms are summed up in Table 2.1.

Table 2.1: Comparison of paradigms

	Workpiece in Machine	**Machine on Workpiece**
Machine Foundation	Large concrete slab.	Workpiece.
Scalability	Not possible.	No upper bound.
Mobility	Low.	High.
Global Referencing	Internal (machine axes).	External.
Loads on workpiece	Clamping and cutting loads.	Machine mass and cutting loads.
Workspace	$\geq$ workpiece size.	= machined volume.

2.3 Problem Definition

The overall goal of this Ph.D. project is development of methods for prediction of obtainable tolerances and optimization of efficiency for the InnoMill machining cell. The predictions will rely on flexible multibody dynamic models of the system.

This report sums up the work carried out from August 2015 to spring 2017. As development of the new machine concept has lasted until the spring of 2017, multibody modelling of the system has not been possible yet. Instead the work is focused on initial feasibility studies and assisting the development of the machine with simple models.

The work consists of two main sections: Workpiece Analysis and Machine Development. Workpiece Analysis covers initial studies of compliance- and dynamic properties of the workpiece case study (Vestas V112-3.0MW hub), and work with model verification. The studies are motivated by the fact that the workpiece will be used to carry the weight of the machine. Therefore, it is considered important to understand the mechanical behaviour of the workpiece. In the Machine Development section the machine concept is presented and details regarding development and modelling of a subsystem of the machine is elaborated. The subsystem is a Stewart-Gough platform (six degree of freedom parallel manipulator), which is used for alignment purposes in the InnoMill machine.

Workpiece Analysis

This chapter covers analysis of the workpiece case study for the InnoMill project, a Vestas V112-3.0 MW hub. The purpose of the analysis is to gain knowledge regarding stiffness- and vibrational behaviour of the workpiece prior to constructing the InnoMill machine and developing tolerance prediction models. In addition, work is done to investigate the validity of the workpiece model.

3.1 Workpiece Case Study

CAD models of the Vestas V112-3.0 MW hub is supplied by Global Castings A/S. In Figure 3.1 the CAD model of the hub before and after machining is shown. The dimensions shown on Figure 3.1a are $Height \approx 3400mm$, $Mainshaft\ Diameter \approx 2400mm$ and $Containing\ Diameter \approx 3600mm$. The weight of the hub is approximately 16 ton before machining, and 14 ton after machining. The full model, as shown in Figure 3.1 is referred to as Model A.
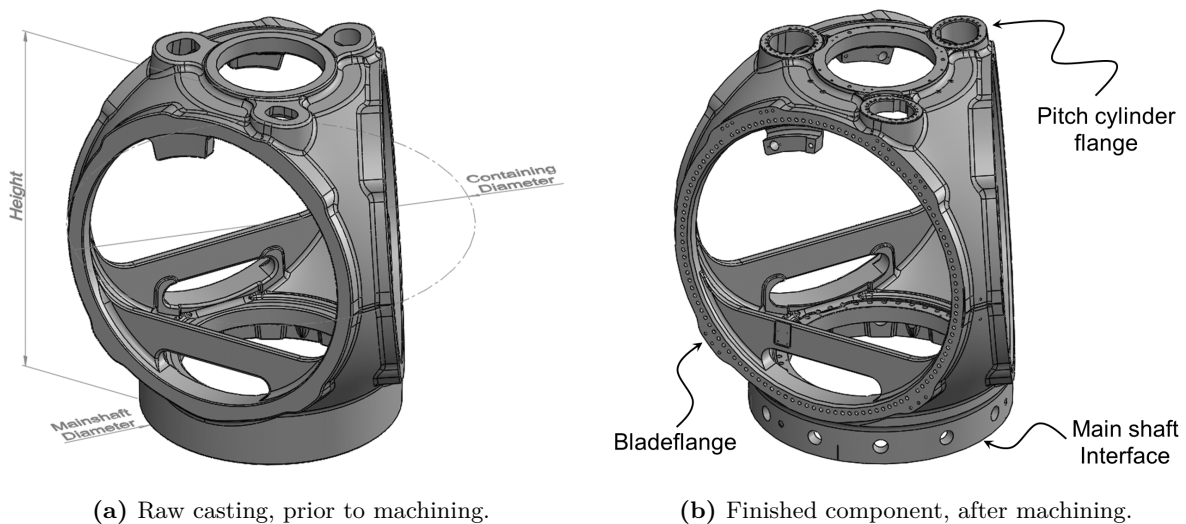

(a) Raw casting, prior to machining.

(b) Finished component, after machining.

Figure 3.1: Workpiece Model A

A simplified model of the unmachined hub without fillets and small details is deviated from model A. The model which is referred to as Model B is shown in Figure 3.2. Dimensions are equal to those of Model A, and the mass of the simplified model is also approximately 16 ton.

Based on information supplied by Global Castings A/S the material parameters used in modelling are Young's Modulus $E = 165GPa$, Poisson's ration $\nu = 0.272$, density $\rho = 7100\frac{kg}{m^3}$, coefficient of thermal expansion $\alpha = 1.212 \cdot 10^{-5}\frac{1}{°C}$, specific heat capacity $c = 450\frac{J}{kg \cdot K}$ and thermal conductivity $\kappa = 25\frac{W}{m \cdot K}$. All material parameters stated are for a temperature of $20°C$.

Factors

During machining with the InnoMill machine multiple effects, which might be different from item to item due to casting tolerances, can lead to deflections of the workpiece. The casting process is conducted using large sand molds. Casting tolerances depends on the item size and according to [8] the tolerances are in the range of 1.6-4 mm. Additionally cores can be slightly
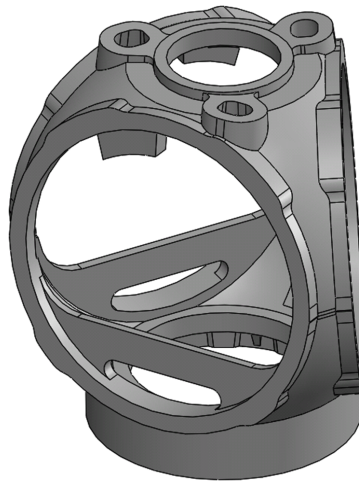
Figure 3.2: Workpiece Model B.

shifted, leading to deviating geometry. Uneven cooling of the melt yields varying micro structure and risk of residual stresses in the items. In the machining setup the boundary conditions of the workpiece has an impact on how the structure deflects and vibrates. During the machining process material is continuously cut of the workpiece, yielding changes of mass- and stiffness properties throughout the process. The workpiece is subjected to both self-weight, weight of the machining cell and cutting loads during the process. Furthermore ambient and local temperature changes in the cutting zone might cause thermal expansion of the workpiece.

Tolerance Requirements

No detailed information regarding tolerance requirements are disclosed in this report, due to the confidentiality of production drawings for the Vestas V112-3.0 MW hub. In general terms, the tolerances are in the range of some millimetres and down to 0.1 millimetres. Both position-, orientation and nominal tolerances are utilized, along with several different geometric tolerances.

3.2   Finite Element Model

Studies of the workpiece is performed using the finite element method, which in general is a method for numerical solution of field problems. For structural problems the method can be utilized for solving e.g. displacement or strain, and any geometry can be analysed. Boundary- and loading conditions are not restricted to special cases, and material properties can be defined as desired [9]. The basic idea of finite element analysis is to discretise a complex continuous problem using a finite number of elements for which mathematical description of the problem is relatively simple. Once the discretised model is obtained it can be used to solve e.g. static linear problems, eigenvalue problems or nonlinear problems. To avoid discretisation dependent solutions it is key to ensure that the discretisation has converged.

Software

The commercial finite element software Abaqus 6.14-3 [10] is used for analysis of the Vestas V112-3.0 MW hub. The mesh is build using three types of three dimensional continuum elements,

which are C3D20R (20-node brick element, reduced integration), C3D15 (15-node wedge element, full integration), C3D10 (10-node tetrahedral element, full integration).

Both static linear analysis, geometrically nonlinear analysis, frequency analysis and transcient coupled thermal-mechanical analysis is conducted using the different solvers available in Abaqus.

Analyses is conducted using the Abaqus Scripting Interface, which is an extension of the Python object-oriented programming language. Both pre- and postprocessing have been performed using Python scripts. Utilising the scripting capabilities of Abaqus enables conducting large parametric studies.

Discretised Models

The high fidelity model (A) is utilized for investigation of validity of the model, see Section 3.4. The simplified model (B) is used for studying the effects presented previously, see Section 3.3. Convergence studies with respect to static- and vibrational response is conducted for model B and a convergence study of vibrational response is conducted for model A.

Illustrations of the converged meshes are shown in Table 3.1, and number of elements and nodes are listed below the figures. In [11] another model of the full geometry (model A) created using ANSYS simulation software yields approximately 900.000 elements. Due to the large number of degrees of freedom the analyses are computationally heavy.

Table 3.1: Finite Element Models of Workpiece

Model A	**Model B**
Detailed Geometry	Simplified Geometry

442,252 elements	164,734 elements
686,116 nodes	263,625 nodes

3.3   Parametric Study

Importance of some of the factors presented in the previous section are investigated using work-piece Model B. The presented work and results are excerpts from a InnoMill milestone report [12], which covers the analysis in depth.

Deflections

Different factors leading to deflections of the hub during machining are studied using parametric studies. The hub is fixed on three surface pads indicated in Figure 3.3. Due to material cutting, the geometry will continuously change throughout the machining process. In these studies machining of one layer of one bladeflange is studied using nine different models for different stages of the process. Deflections of the toolpoint positions for the nine models are compared to tolerance requirements for the bladeflange regarding flatness and accuracy of hole positions. The main findings of the studies are listed below

Geometric nonlinearity:	By comparison of linear- and geometric nonlinear analysis it is found that linear analysis is adequate.
Machine- and selfweight:	Weight of the hub and up to 10 ton of machine weight placed symmetrically or asymmetrically does not cause deflections exceeding the tolerance requirements.
Cutting Forces:	Two perpendicular forces of each 5000 N applied at the cutting zone does not yield critical deflections.
Cutting Heat input:	Currently no adequate model of cutting heat input is available, hence no conclusions are made regarding the topic.
Ambient Temperature:	Increasing the temperature of the hub from $20°C$ to $40°C$ yields deflections exceeding the tolerances. Therefore control of ambient temperature or compensation for thermal expansion is important.

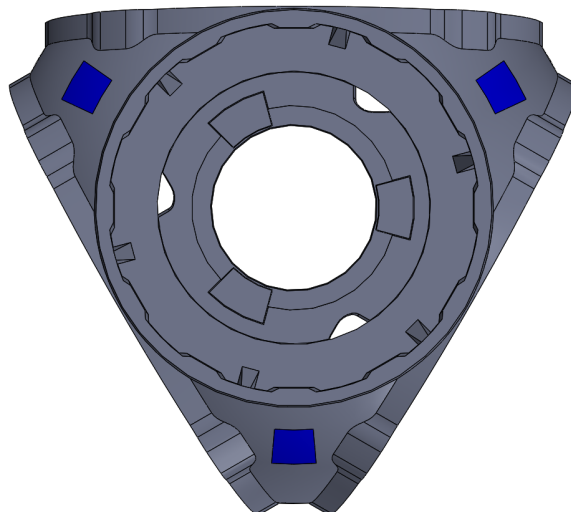**Figure 3.3:** View from hub main shaft interface. Fixed boundary condition regions marked in blue.

Vibrational Response

Knowledge of vibrational response of the workpiece is key to ensure stable and efficient cutting [2, 3, 5]. Utilising model B different studies are made to gain insight regarding vibrational response of the Vestas V112-3.0 MW hub main conclusions are listed below

Boundary Conditions:	As expected, fixture boundary conditions are important to the vibrational response.
Cutting Process Frequencies:	Several natural frequencies exist in the range $0 - 200 Hz$, which is the expected forcing frequency range of the cutting processes.
Material Removal:	Changes of natural frequencies caused by milling of the hub are relatively small [11, 12]. For the ten first frequencies the changes are below 2 per cent for approximately 7.5 per cent of the total hub mass removed.

3.4 Validity

The validity of the finite element model vibrational response is investigated by comparison to vibrational response measured using Operational Modal Analysis (OMA) techniques.

Experiments

Experiments are conducted by Ph.D. student Martin Juul and M.Sc. student Emese Kovàcs from civil engineering [13, 14] and a brief resume is given here. The Vestas V112-3.0 MW hub is placed on six equally spaced polyurethane blocks, see Figure 3.4a. 20 uniaxial accelerometers are placed on the hub and a OMA measurement series is conducted. 14 sensors are moved to new sensor positions and another measurement is made. The cycle continues until all 63 sensor positions on the hub are covered. Six sensors serve as reference sensors to allow merging of the different test series. Sensor positions and directions are illustrated in Figure 3.4b. After data processing natural frequencies and mode shapes of the hub are obtained.

Finite Element Model

The full model (Model A) is utilised for the validity study. The polyurethane blocks supporting the hub are modelled using three linear springs, in x, y and z directions respectively. Spring stiffnesses in the plane parallel to the floor (k_x, k_y) are assumed to be equal, and spring stiffnesses are assumed to be equal for all six supports. Modal analysis is performed using Abaqus Frequency, and the mode shapes are exported for the 63 sensor positions. The mode shapes from Abaqus are described in x, y, z coordinates, and are therefore not directly comparable to the experimental mode shapes which are expressed in terms of surface normal directions. To ensure comparability the finite element mode shapes are projected onto the sensor normal directions, yielding mode shape vectors with 63 degrees of freedom.

Comparison

The experimental mode shapes and the modelled mode shapes are compared using the Modal Assurance Criteria (MAC) [15] which basically expresses whether mode shapes coincide.

Model A and the experimental results are compared for a large variety of model support spring stiffnesses. Initially only four mode shapes shows reliable identification ($MAC = 1$
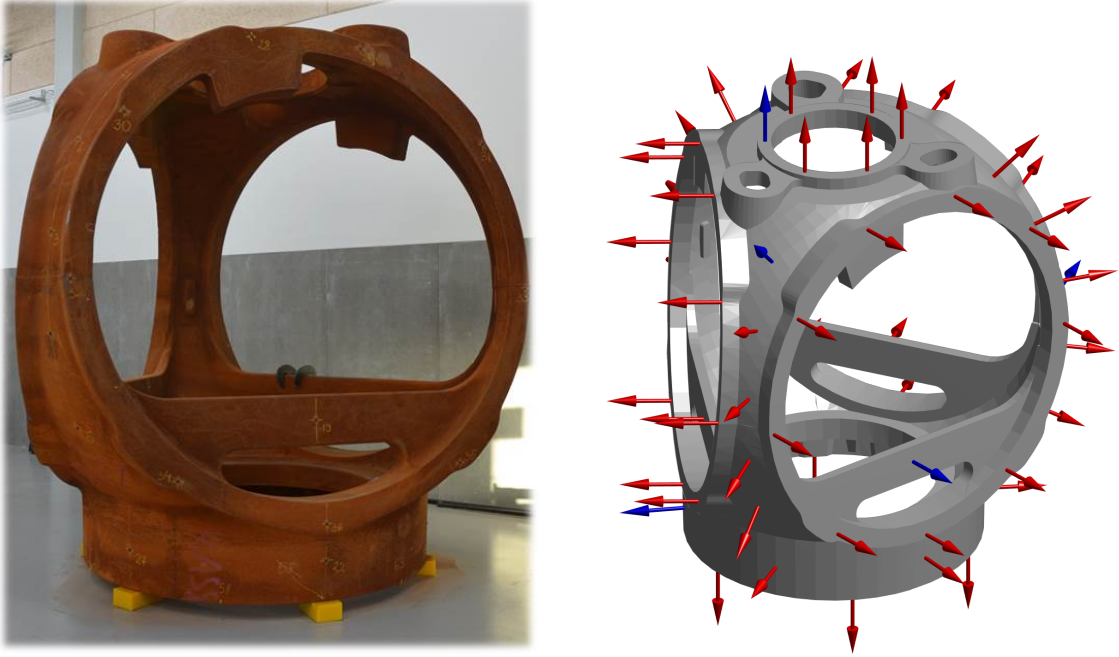
(a) Hub Vibrational Measurement Setup. Yellow supports are polyurethane blocks and some sensor positions (marked with crosses and numbers) can be seen.

(b) Visualisation of sensor poisitions and directions. Blue markers are fixed reference sensors.

Figure 3.4: Vibrational Experimental Setup of Vestas V112-3.0 MW hub.

means a full match of mode shapes). The four mode shapes are picked out, and the MAC values are used in the cost function of Equation 3.1 which goes to zero when the experimental results equals the model results.

$$J(k_x, k_z) = \sum_{m=1}^{4} 1 - MAC(\mathbf{a}_m, \mathbf{b}_m(k_x, k_z)) \tag{3.1}$$

$\mathbf{a}_m$ denote current mode shape from experiments and $\mathbf{b}_m(k_x, k_z)$ denote current mode shape for given support spring stiffnesses of finite element model A.

The resulting functional values shown in Figure 3.5 show a clear tendency of the free version (zero stiffness of boundary springs) being appropriate for description of vibrational response of the hub placed on polyurethane blocks.

By investigation of experimental- and model A results it is found that the incapability of successful identification is caused by a lack of compensation for closely spaced modes [16]. Closely spaced modes can be identified by frequencies being almost equal for two modes. For structural dynamics eigenvectors associated with identical eigenvalues are not unique, hence any linear combination of the two eigenvectors is also an eigenvector. Therefore the closely spaced modes can be considered to span a plane in which all vectors are essentially valid mode shape vectors. Juul et. al. [16] utilises this realisation, and rotates the experimental closely spaced modes in their plane to a best-fit match with the finite element mode shapes. Implementation of the method on individual datasets yield the MAC plot shown in Figure 3.6, which shows good correlation for mode shape 1 to 17.

Based on the good correlation it is concluded that finite element model A of the hub is discretised adequately, and that material parameters used are realistic. Furthermore, polyurethane blocks serve as good vibrational isolation for items of this size.
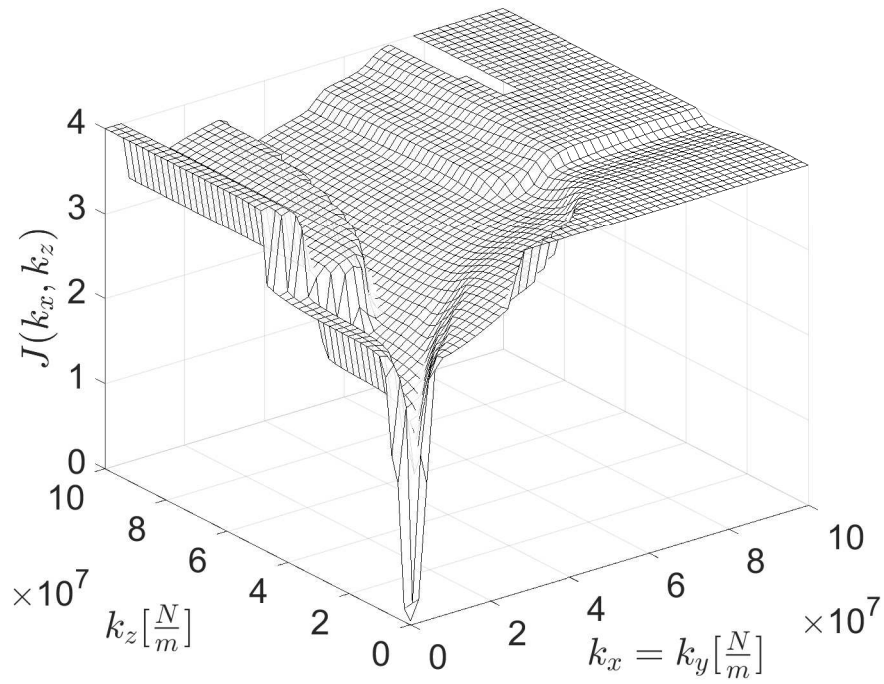
Figure 3.5: Functional values of Equation 3.1. Figure from [16].
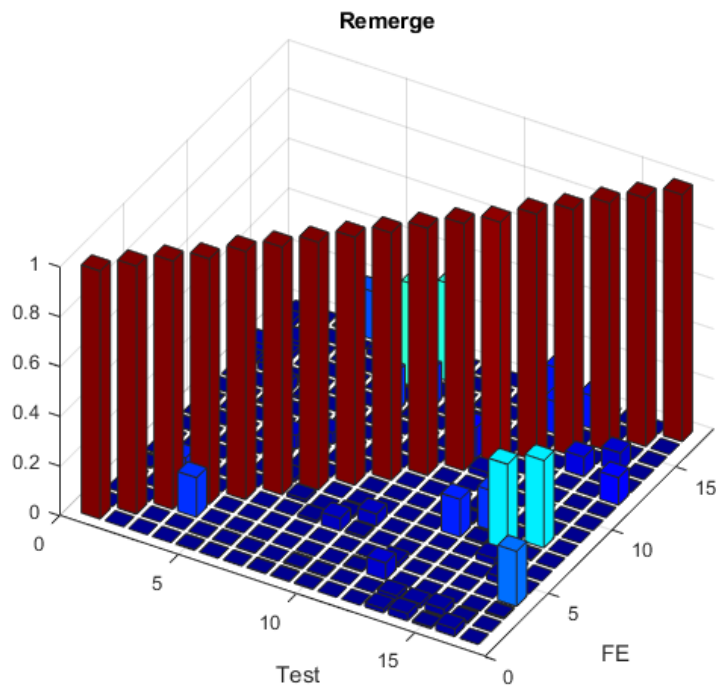

Figure 3.6: Final MAC value between experimental- and Model A mode shapes. Figure from [16].

Machine Development

The basic idea of the InnoMill machine concept is presented in this chapter, and different machine architectures are discussed. A subsystem of the machine consists of a Stewart-Gough platform (six degree of freedom parallel manipulator), for which basic theory is presented. A method for including base elasticity during design of the Stewart-Gough platform is proposed and tested on a case study. Furthermore, a spring-mass model for prediction of vibrational response of the Stewart-Gough platform is proposed. The mode shapes obtained from the model are compared to experimental results to asses the performance of the model.

4.1 Concept Description

A basic concept is synthesised based on concept development and selection in the InnoMill project group. The machine is attached to the workpiece, and consists of an alignment mechanism, a three degree of freedom (dof) serial kinematic CNC machine and an external referencing system, see Figure 4.1. The three dof CNC machine is designed as a RPP (Rotational-Prismatic-Prismatic) mechanism yielding planar machining operations in a cylindrically shaped workspace. Kinematics and dynamics of the CNC machine for simulation and control purposes can be derived using Denativ-Hartenberg parameters [17].
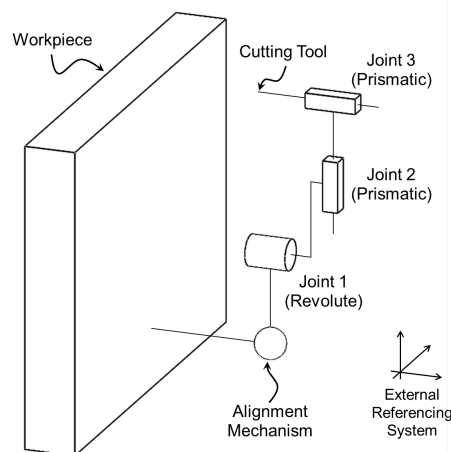

Figure 4.1: Conceptual sketch of InnoMill machine

The workflow of using the machine is; Reference the workpiece with respect to the external referencing system, attach the InnoMill machine to the workpiece and reference it, use the alignment mechanism to align the CNC machine to the desired plane and lock it, run machining programme. When the CNC machine is done the alignment mechanism can realign the CNC machine to reach new features or the entire machine can be relocated to a new position on the workpiece. Referencing is required in either case. Alignment of the CNC machine is conducted prior to machining operations to avoid controlling all five axes during machining operation.

Alignment Mechanism

Only five dof are required to perform spatial machining operations, due to the fact that the rotary axis of the spindle is the sixth dof. To allow the machine to have three translational and

two rotational dof in total, the alignment mechanism must provide two rotational dof.

Two different mechanism architectures are applicable for the alignment mechanism: Serial-and Parallel Kinematic. Some important characteristics of the two manipulator architectures are summed up in Table 4.1.

Table 4.1: Manipulator characteristics [18, 19, 20, 21]

	Serial kinematic Figure 4.2a	**Parallel kinematic** Figure 4.2b
Position Error	Accumulates	Averages
Stiffness	Low	High
Dynamic Characteristics	Poor (Large inertia)	Good (Small inertia)
Workspace	Large	Small
Uniformity of Components	Low	High
Calibration	Relatively Simple	Complicated
Payload/weight ratio	Low	High

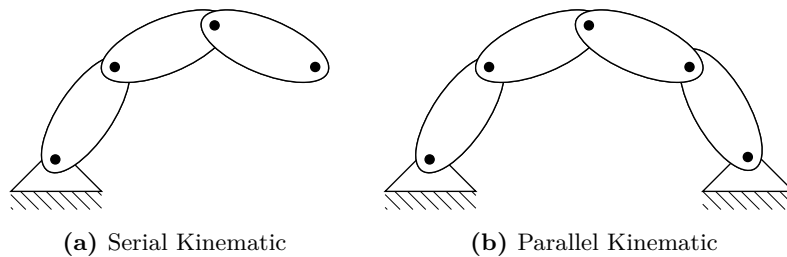**(a)** Serial Kinematic   **(b)** Parallel Kinematic

Figure 4.2: Basic Manipulator Architectures

Parallel manipulators have been successfully utilised for precision positioning tasks in e.g. lab equipment, space industry and manufacturing [18, 21]. Combination of high accuracy, high stiffness and high payload-to-weight ratio are some of the main motivations for choosing a parallel kinematic architecture for the alignment mechanism of the InnoMill machine. Combining the parallel kinematic alignment mechanism with the serial kinematic CNC machine makes the InnoMill machine a hybrid structure, which according to [18] is successfully used for machining purposes.

Parallel Manipulator

Development and design of parallel manipulators is of great interest to academia. Different researchers have synthesised various architectures of which some are applicable for the InnoMill alignment mechanism. The requirements for the InnoMill alignment mechanism are; the mechanism must provide minimum two rotational degrees of freedom, the workspace between the struts is preferably free to allow the CNC machine to be mounted as illustrated in Figure 4.3, low weight and high stiffness is important.

Different researchers [22, 23, 24] proposes three-degree-of-freedom fully rotational parallel manipulators for e.g. wrist joints and camera orientation devices. The mechanism provide a large rotational workspace, and parasitic translational motion occurs. The struts consists of curved members which are subjected to bending moments. Utilisation of the workspace between the struts is infeasible due to the complex architecture of the curved members.

Among others Lee et. al [25] studies a three-degrees-of-freedom in-parallel manipulator consisting of three RPS (Revolute, Prismatic, Spherical) chains connected to one moving platform.
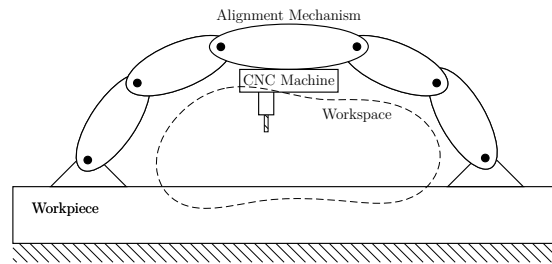
Figure 4.3: InnoMill CNC machine on parallel manipulator alignment mechanism.

The 3-R$\underline{\text{P}}$S architecture has two rotational and one translational (heave) dof. During rotational motion of the platform, parasitic translational motion occurs. The primatic actuators and the revolute joints are subjected to bending moments.

Another three-degree-of-freedom manipulator which has three active U$\underline{\text{P}}$S chains (Universal, Prismatic, Spherical) and one passive FPU (Fixed, Pristmatic, Universal) chain mounted at the center of the manipulator is proposed by Fattah and Kasaei [26]. The manipulator has two rotational and one translational (heave) dof. The central strut ensures that no parasitic translational motion occurs when rotating the platform, but it has to withstand bending moments. Furthermore, utilisation of the workspace between the struts is not possible due to the fixed central passive strut.

Another parallel architecture capable of providing two rotational dof is the six dof Stewart-Gough platform which was initially developed by Gough [27]. The platform consists of six identical struts, each consisting of S$\underline{\text{P}}$S (Spherical, Prismatic, Spherical), U$\underline{\text{P}}$U (Universal, Prismatic, Universal) or similar architectures. The architecture ensures pure axial forces in the struts (assuming no friction in the joints), and allows full control of three rotational, and three translational dof in a relatively small and complex workspace.

Based on findings presented in this section, the InnoMill project group decides to continue machine development based on a six dof Stewart-Gough platform alignment mechanism. The main arguments for continuing in this direction are; six actuators in pure tension/compression is expected to be lighter and cheaper than three actuators in bending; having six struts provides design freedom when choosing where to attach the machine to the workpiece; redundant dof provides more universal usage and possibility of minimisation of deflections for a given pose (a given pose can be reached in multiple ways).

4.2 Stewart-Gough Platform

A Stewart-Gough platform basically consists of a fixed base, a moveable platform and six kinematic chains connecting the two parts, see Figure 4.4. In the InnoMill case the fixed base consists of six attachment points on the workpiece, and the moveable platform carries the three dof CNC machining unit. Geometrically the mechanism can be described using the two reference frames {$\mathbf{A}$} and {$\mathbf{B}$} fixed on the workpiece and the moveable platform respectively.

Kinematics

Working with robotic manipulation two types of kinematics are of interest; Inverse- and Forward-kinematics.

Inverse kinematics covers solving jointspace coordinates based on given taskspace coordinates. For the Stewart-Gough platform position $^A\mathbf{P}$ and orientation $^A\mathbf{R}_B$ of the moveable platform are given (taskspace), and actuator lengths are solved $\mathbf{L} = [l_1, l_2, l_3, l_4, l_5, l_6]^T$ (jointspace).
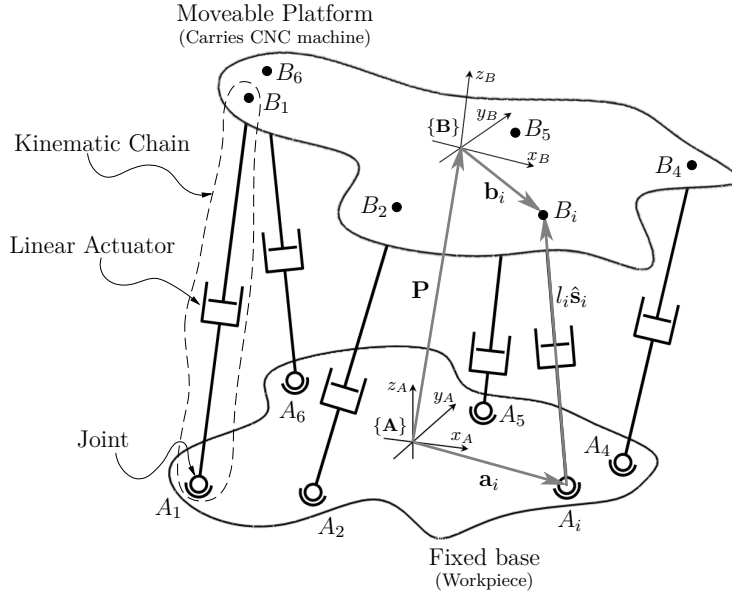
Figure 4.4: Schematic of Stewart-Gough platform.

The solution is found using the Loop-Closure method, which is initialised by writing the loop closure equation for each strut, $i = 1, 2, \ldots, 6$ for point $\mathbf{B}_i$, and isolating the actuator vector $l_i \hat{\mathbf{s}}_i$.

$$^A\mathbf{a}_i + l_i{}^A\hat{\mathbf{s}}_i = {}^A\mathbf{P} + {}^A\mathbf{R}_B{}^B\mathbf{b}_i \tag{4.1}$$

$$l_i{}^A\hat{\mathbf{s}}_i = -{}^A\mathbf{a}_i + {}^A\mathbf{P} + {}^A\mathbf{R}_B{}^B\mathbf{b}_i \tag{4.2}$$

where vectors are shown in Figure 4.4. $\hat{\mathbf{s}}_i$ is a unit vector describing the direction of the strut i.

Forward kinematics is opposite to inverse kinematics, meaning solving taskspace coordinates based on given jointspace coordinates. For a Stewart-Gough platform given a vector of actuator lengths, $\mathbf{L} = [l_1, l_2, l_3, l_4, l_5, l_6]^T$, the task is to solve the pose of the moveable platform, $^A\mathbf{P}$ and $^A\mathbf{R}_B$. For any given vector of joint coordinates multiple solutions exists, hence a closed loop solution is not possible for the general manipulator [20]. Instead forward kinematics can be solved using numerical procedures e.g. nonlinear least-squares optimization routines. Successful implementation of such routines requires small motion steps and adequate convergence criteria.

Jacobian Analysis

Differential kinematic analysis of Stewart-Gough mechanisms leads to derivation of the Jacobian matrix. In robotics Jacobian matrices are utilised for velocity, static force, stiffness and singularity analysis. The Jacobian matrix is derived by differentiation of Equation 4.1 with respect to time, which yields

$$^A\dot{\mathbf{a}}_i + \dot{l}_i{}^A\hat{\mathbf{s}}_i + l_i{}^A\dot{\hat{\mathbf{s}}}_i = {}^A\dot{\mathbf{P}} + {}^A\dot{\mathbf{R}}_B{}^B\mathbf{b}_i + {}^A\mathbf{R}_B{}^B\dot{\mathbf{b}}_i \tag{4.3}$$

Since $^A\mathbf{a}_i$ and $^B\mathbf{b}_i$ are fixed lengths their time derivatives are zero. Following some calculation the Equation 4.3 can be written as

$$^A\hat{\mathbf{s}}_i{}^A\mathbf{v}_B + ({}^A\mathbf{b}_i \times {}^A\hat{\mathbf{s}}_i){}^A\boldsymbol{\omega} = \dot{l}_i \tag{4.4}$$

where $^A\mathbf{v}_B = [\dot{x}_B \quad \dot{y}_B \quad \dot{z}_B]^T$ is the velocity of the moving platform expressed in reference frame $\{\mathbf{A}\}$ and $^A\boldsymbol{\omega}$ is the rotational velocity of the platform expressed in reference frame $\{\mathbf{A}\}$. By assembling Equation 4.4 for $i = 1, 2, \ldots, 6$ in matrix format, the Jacobian matrix is defined as

$$\mathbf{J} = \begin{bmatrix} \hat{\mathbf{s}}_1^T & (\mathbf{b}_1 \times \hat{\mathbf{s}}_1)^T \\ \hat{\mathbf{s}}_2^T & (\mathbf{b}_2 \times \hat{\mathbf{s}}_2)^T \\ \vdots & \vdots \\ \hat{\mathbf{s}}_6^T & (\mathbf{b}_6 \times \hat{\mathbf{s}}_6)^T \end{bmatrix} \tag{4.5}$$

where all vectors are expressed in reference frame $\{\mathbf{A}\}$. Superscript A is omitted for readability.

Singularities of Stewart-Gough platforms can have one of two physical consequences; Instantaneous loss of one degree of freedom leading to a loss of controllability or degradation of stiffness which can cause joint forces to increase severely. Singular configurations occur if the Jacobian matrix becomes rank deficient, which is the case when the matrix determinant approaches zero $(det(\mathbf{J}) \approx 0)$.

Static forces in actuators under some static wrench applied to the Stewart-Gough platform are calculated using the Jacobian matrix by the following equation

$$\mathbf{F} = \mathbf{J}^T \boldsymbol{\tau} \tag{4.6}$$

where $\mathbf{F} = [\mathbf{f}, \mathbf{n}]^T$ is a vector of external forces and torques on the moveable platform, at the reference frame $\{\mathbf{B}\}$ and $\boldsymbol{\tau}$ is a vector of axial forces exerted by the actuators.

Additionally, static deflections of the moveable platform caused by axial deflections of the actuators can be computed using the Jacobian matrix. The stiffness matrix is calculated from

$$\mathbf{K} = \mathbf{J}^T \boldsymbol{\kappa} \mathbf{J} \tag{4.7}$$

where $\boldsymbol{\kappa}$ is a diagonal matrix containing axial stiffness of actuator $i = 1, 2, \ldots 6$ on entry $\boldsymbol{\kappa}_{ii}$. By inverting the stiffness matrix $\mathbf{K}$ the compliance matrix $\mathbf{C}$ is obtained. Utilising the compliance matrix the deflections of the moveable platform are computed from

$$\Delta\mathbf{X} = \mathbf{C}\mathbf{F} \tag{4.8}$$

where $\Delta\mathbf{X} = [\Delta x \quad \Delta y \quad \Delta z \quad \Delta\theta_x \quad \Delta\theta_y \quad \Delta\theta_z]^T$ is the vector of translational and rotational deflections of the reference frame $\{\mathbf{B}\}$ described in frame $\{\mathbf{A}\}$.

Furthermore multiple performance indices which are often used in optimisation of Stewart-Gough platforms are directly related to the Jacobian matrix of the manipulator [19, 20].

Dynamics

Dynamics of the Stewart-Gough platform can be derived using multiple different methods. General purpose multibody dynamic formulations such as constraint-based Cartesian formulation [28] leads to a model containing 13 bodies, leading to 78 degrees of freedom in total. Compared to single-body special purpose methods, as discussed by Taghirad [20], the computational performance of the Cartesian formulations is poor. Single body dynamic formulations are derived using Newton-Euler, Principle of Virtual Work or Lagrange formulations. Dynamic simulation of the Stewart-Gough platform is not applied in this project, since motion of the platform are slow to ensure accuracy. Therefore, dynamic modelling of the Stewart-Gough platform is not discussed in detail in this report.

4.3   Stewart-Gough Platform on Elastic Base

Research on Stewart-Gough platforms assume a rigid fixed base as a prerequisite for analysis of accuracy, workspace, deflections and other performance indices. For the InnoMill project the base of the Stewart-Gough platform (workpiece) is in general not a rigid body, hence existing analyses are insufficient. This section introduces base elasticity in Stewart-Gough platform performance analysis, and discusses the importance of base elasticity for Stewart-Gough mechanisms. Base elasticity is included using an additional vector, $\boldsymbol{\delta}\mathbf{a}_i$, see Figure 4.5. Including the extra term Equation 4.1 is alternated to

$$^A\mathbf{a}_i + {}^A\boldsymbol{\delta}\mathbf{a}_i + l_i'{}^A\hat{\mathbf{s}}_i' = {}^A\mathbf{P} + {}^A\mathbf{R}_B{}^B\mathbf{b}_i \tag{4.9}$$

for $i = 1, 2, \ldots, 6$. Primes denotes terms which are different from Equation 4.1 and Figure 4.4.

The base deflection terms $\boldsymbol{\delta}\mathbf{a}_i$ are dependent on the base stiffness and actuator force directions and magnitudes. The actuator forces are dependent on the Jacobian matrix $\mathbf{J}$, which is dependent on the pose of the moveable platform, which is dependent on the loop closure chain which involves the deflection term. Therefore, derivation of a closed loop solution is not straight forward for the general case.
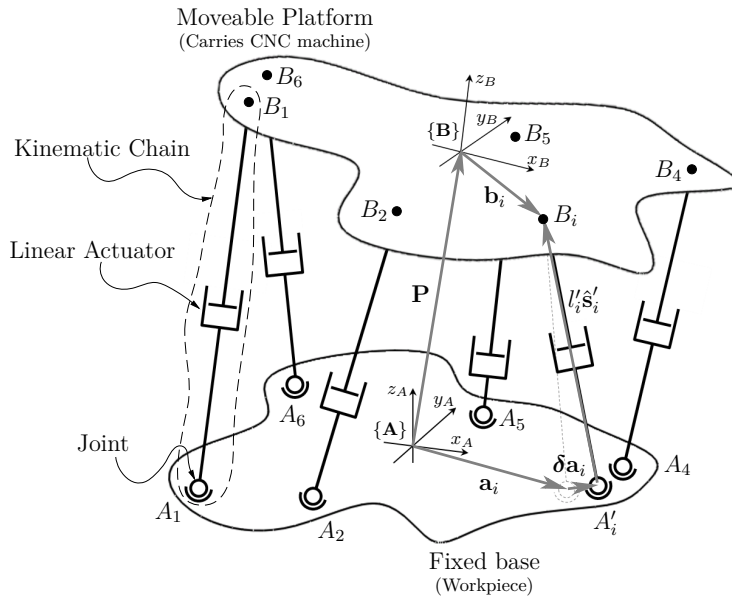

Figure 4.5: Loop Closure with deflection of base. Deflection is only visualised for one strut.

Iterative Solution

An iterative procedure is proposed for determining static equilibrium, and solving the kinematics of the Stewart-Gough platform on elastic base. Two different starting points for the analysis can be taken, depending on whether the purpose of analysis is to correct or to predict the toolpoint position and orientation error.

Case A: If the purpose is to correct actuator lengths l_i to obtain a certain pose of the moveable platform the inverse kinematics stated in Equation 4.9 can be used in an iterative procedure where the actuator lengths are corrected for each step. This approach can be used for correcting the programmed actuator lengths of the Stewart-Gough platform before usage.

Case B: In the case that rigid body assumptions are used when programming the Stewart-Gough platform an elastic base will cause lack of accuracy. If the purpose of the analysis is to investigate whether the magnitude of error is acceptable, the study is conducted under the assumption of fixed actuator lengths l_i. This type of analysis require forward kinematic analysis using e.g. nonlinear least-squares optimization.

Additionally, if the desired toolpoint pose is attached to the deflecting base, the deflections of the toolpoint also have to be accounted for in either of the two cases mentioned. For both cases the Stewart-Gough platform performance, such as workspace and singularities, can be determined for the deflected structure. Algorithm 1 shows the main structure of the iterative procedure.

> **Input**: $^A\mathbf{P}$ and $^A\mathbf{R}_B$
> **while** *error* $> \epsilon$ **do**
> | Compute Jacobian matrix $\mathbf{J}$ based on current pose;
> | Compute static actuator forces from $\boldsymbol{\tau} = \mathbf{J}^{-T}\mathbf{F}$;
> | Compute deflection vectors $^A\boldsymbol{\delta}\mathbf{a}_i$ from e.g. a finite element model;
> | Update variable parameter using either inverse or forward kinematics (depending on
> | purpose of analysis);
> | Evaluate *error*;
> **end**
> **Output**: Kinematics of deflected Stewart-Gough platform

Algorithm 1: Iterative procedure for computation of kinematics for a Stewart-Gough platform on an elastic base.

Test Case

A test case is studied to emphasise the importance of including base elasticity for Stewart-Gough platform simulation. The test follows Case B, where actuator lengths are fixed throughout the equilibrium loop. The example is illustrated in Figure 4.6, where the base consists of beam elements of circular cross section with radius $r_{beam} = 0.025m$, Young's Modulus $E = 210GPa$, and Poisson's Ratio $\nu = 0.3$. The Stewart-Gough platform moveable platform has radius $r_{MP} = 0.75m$, and is positioned at height $h = 0.5m$ above the base. For the analysis the rotational pose of the platform is computed from Bryant angles of $[\theta_x \quad \theta_y \quad \theta_z]^T = [8° \quad 12° \quad 5°]^T$, and the platform is swept from $-1m$ to $1m$ in the XY-plane of the moveable platform in steps of $0.1m$. A static load of $1000N$ is applied in the x-direction of the moveable platform, and the stiffness matrix of the base is computed using Abaqus 6.14-3 [10].

Determinant of the Jacobian matrix is compared for the rigid base assumption and the elastic base assumption, see Figure 4.7. The result illustrates that the changes of the Jacobian matrix is nonlinear, hence it is tedious to predict the effect of the elastic base without including it in the analysis. The plot also shows that even for a small force of $1000N$ the Jacobian matrix changes above 1 per cent for some of the configurations tested. Furthermore changes of actuator force magnitudes are nonlinear and exceed 1 per cent, and toolpoint positions errors of up to $4mm$ are observed for the analysis. Toolpoint position error and actuator force also changes nonlinearly over the workspace investigated. The test case illustrates that base elasticity might be important when evaluating performance of the InnoMill machine.
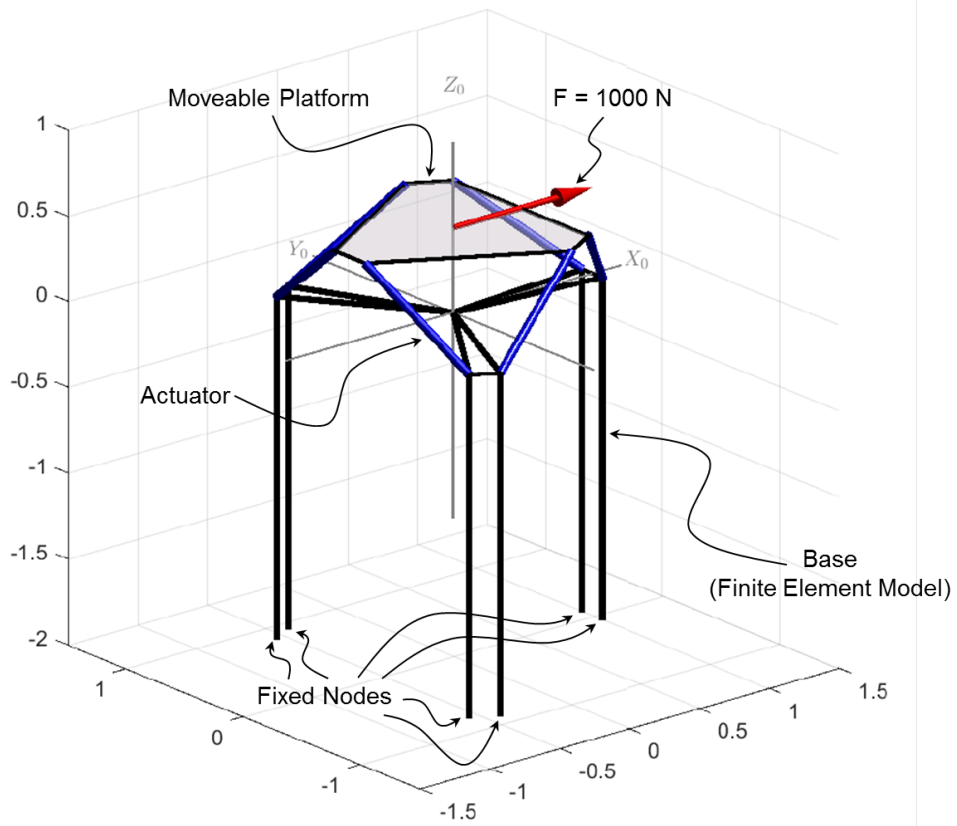
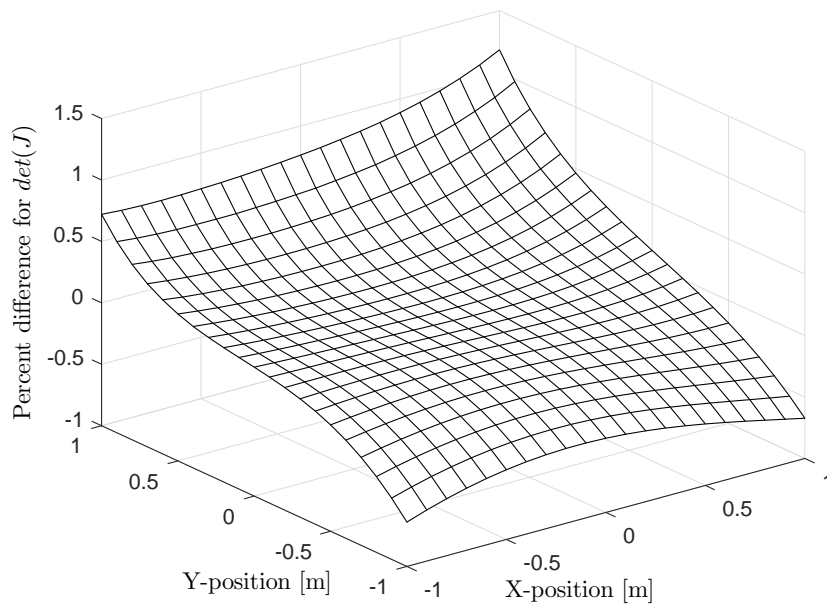**Figure 4.6:** Stewart-Gough platform on elastic base test case.

Figure 4.7: Changes in $det(\mathbf{J})$ for elastic vs. rigid base assumption.

4.4   Modal Analysis of Stewart-Gough Platform

A realistic model including mass and stiffness of the Stewart-Gough platform is required to ensure accurate vibrational stability predictions for the InnoMill machine. In this section a spring-mass model is proposed, and vibrational mode shapes are compared to experimentally determined mode shapes of a Stewart-Gough platform.

Spring-Mass Model

A six dof spring-mass model is derived combining the theory presented in Section 4.2 and [29]. The model assumes rigid base and rigid moveable platform, actuator masses are assumed to be negligible and only axial stiffness of the actuators are considered. An illustration of the model is shown in Figure 4.8. These assumptions allow description of the mass matrix from the inertial matrix of the moveable frame, and a stiffness matrix described by axial stiffness of the six actuators transformed to task space using the Jacobian matrix. Vibrational response of the Stewart-Gough platform is dependent on current pose of the platform, and axial stiffness of the actuators depend on current length.
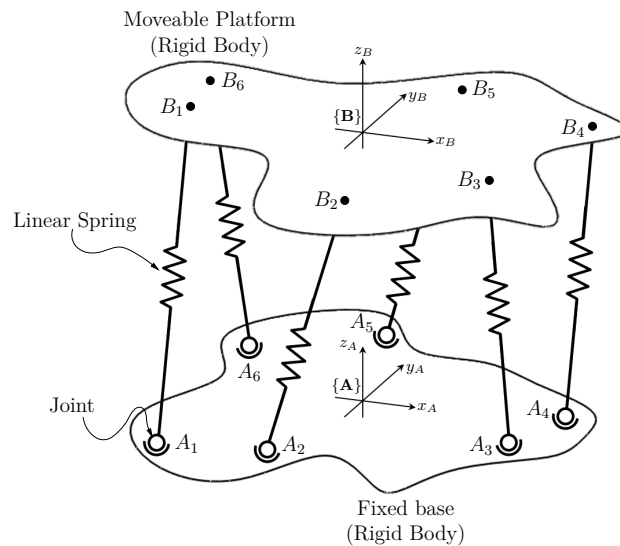

Figure 4.8: Six dof Stewart-Gough platform Spring-Mass model.

For a Stewart-Gough platform with hexagon shaped base and moveable platform positioned in neutral position (no translation or rotation of the platform) the six mode shapes determined using the six dof spring-mass model are described in Table 4.2. Axial stiffness of actuators are assumed to be identical for all six actuators. Frequencies of mode shape 1,2 and 5,6 are identical ($\omega_1 = \omega_2$, $\omega_5 = \omega_6$) due to the rotational symmetry of the Stewart-Gough platform in neutral position, hence the modes are closely spaced.

Experiments

The performance of the six dof spring-mass model is evaluated by comparison to a OMA experiment conducted on a Stewart-Gough platform situated at the Department of Engineering at Aarhus University. Experiments are conducted by Ph.D. student Martin Juul and M.Sc. student Anders Olsen from Civil Engineering. The Stewart-Gough platform is designed for motion simulations, and is produced by MOOG. The product type is MB-E-6DOF/24/1800KG, and

Table 4.2: Mode Shapes of Stewart-Gough platform six dof spring-mass model. Axis refers to reference frame {**B**} of Figure 4.9a. Frequencies are normalised with respect to the first natural frequency.

Mode shape	Description	Normalised Frequency
1	Translation along Y-axis, rotation around X-axis.	1.0
2	Translation along X-axis, rotation around Y-axis.	1.0
3	Rotation around Z-axis.	1.9
4	Translation along Z-axis.	2.2
5	Rotation around Y-axis and X-axis.	3.0
6	Rotation around X-axis and Y-axis.	3.0

the machine in the experimental setup is shown in Figure 4.9b. 18 uniaxial accelerometers are placed on the moveable platform and two on the sides of one of the actuators. The Stewart-Gough platform is excited both manually and using four electromechanical exciters, and data is collected and processed to obtain natural frequencies and mode shapes of the structure.

Excitation using exciters is efficient and easy, but results depend on where the exciters are mounted on the Stewart-Gough platform. Consistent results are obtained if exciter positions are not changed. Manual excitation is currently conducted by three persons brushing the surfaces of the Stewart-Gough platform using steel brushes for three minutes, hence the method is labour intensive. Consistency of results from manual excitation has not been documented for the time being.
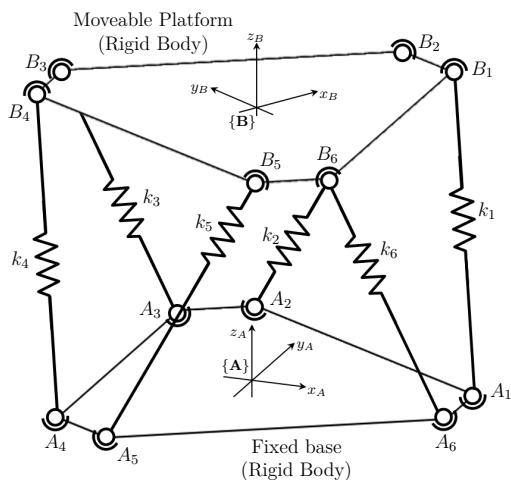
(a) Six dof Stewart-Gough platform Spring-Mass model of MOOG Motionbase.

(b) MOOG MB-E-6DOF/24/1800kg at Aarhus University.

Figure 4.9: Stewart-Gough Platform Vibrational Response Experiment

Comparison

Based on comparing animated mode shapes obtained from experiments and the model presented, the general conclusion is that the six dof spring-mass model does not contain enough dof to realistically mimic the vibrational response of the real structure. Mode shapes obtained from experimental results shows lateral deflections of the actuator investigated and structural deflections of the moveable platform, see Figure 4.10 and 4.11.
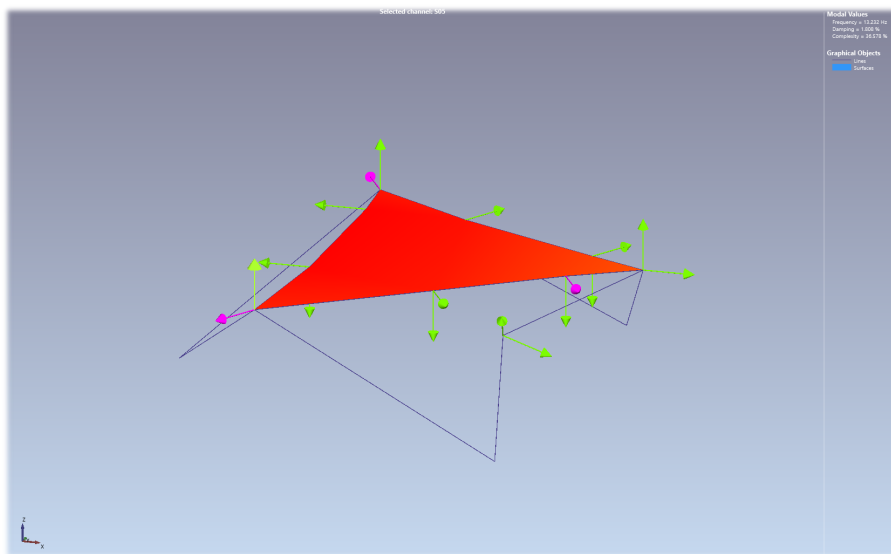
Figure 4.10: Moveable platform "rigid body" mode shape. Animated mode shape provided by Anders Olsen and Martin Juul.
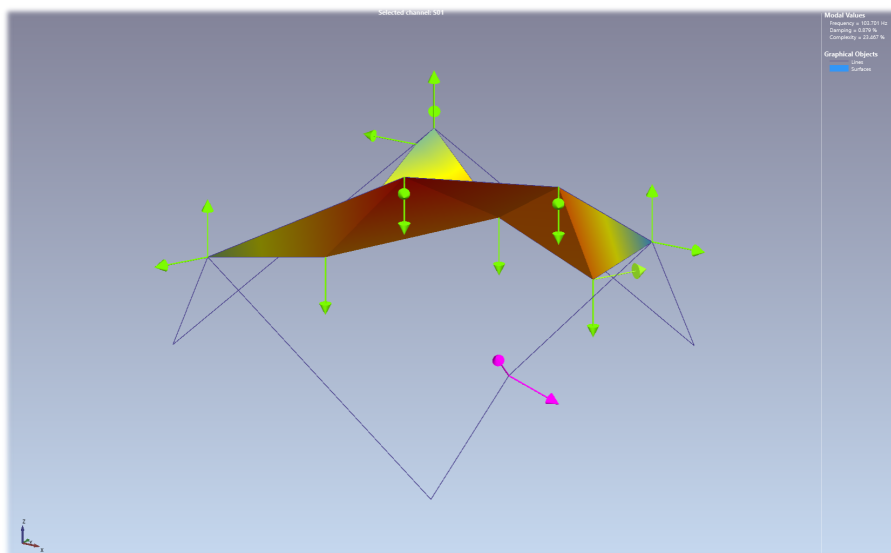

Figure 4.11: Moveable platform flexing mode shape. Animated mode shape provided by Anders Olsen and Martin Juul.

Conclusion

The InnoMill project goal is to develop a competitive mobile and reconfigurable machining cell for manufacturing of large wind turbine components. The machine has to follow the paradigm *"Machine On Workpiece"*. The gain is a scalable system capable of machining even larger components than currently available without requiring investment in new expensive CNC machines. The trade-off might be inefficient machining and problems in complying with tolerance requirements.

Finite element analysis of the InnoMill workpiece case, the Vestas V112-3.0 MW hub, has been conducted to gain insight regarding stiffness- and vibrational properties of the structure prior to developing the machining cell. Static stiffness analysis indicates capability of supporting approximately 10 tonne of machine weight in an asymmetric setting, without deflections exceeding a subset of the tolerance requirements. Cutting forces of 2x5000 N does not yield excessive deflections either. Temperature variations of the workpiece are found to be important, hence either temperature control or compensation should be implemented for the new solution. The vibrational response of the workpiece is analysed, and several natural frequencies are present in the range of the expected forcing frequency of the cutting process. Changes of vibrational response of the workpiece caused by material removal are negligible. Comparing vibrational response of the finite element model to Operational Modal Analysis experimental results has provided indications that discretisation and material parameters used in workpiece modelling are realistic.

The InnoMill machine concept consists of four main components; 1. The workpiece which serves as machine foundation, 2. An alignment mechanism which is a six degree of freedom parallel kinematic Stewart-Gough manipulator, 3. A three degree of freedom serial kinematic CNC machine consisting of one rotational axis and subsequently two translational axes and 4. an external referencing system. The alignment mechanism is adjusted prior to machining, hence only axes of the serial kinematic CNC machine move during machining. Redundancy of axes can be utilised for optimisation of the process and provides additional freedom in the planning of production using the machine.

A iterative solution is proposed and implemented for evaluation of Stewart-Gough platform performance taking elasticity of the base into consideration. Application on a test case show nonlinear changes of performance. Therefore it is concluded that including workpiece elasticity is important during development of the InnoMill alignment mechanism.

Furthermore, a six degree of freedom spring-mass vibrational model of a general Stewart-Gough platform is proposed. The model includes axial stiffness of actuators and the inertia of the moveable platform. Comparison of the proposed model to experimental results has disclosed model incapability of mimicking complex vibrational mode shapes of the MOOG Motionbase at Department of Engineering, Aarhus University. Visual comparison of experimental and model mode shapes highlights the importance of lateral vibration of actuators, and flexibility of the moveable platform.

Outlook

This report present some of the different challenges that is considered during development of the InnoMill machine as a part of Part A of this Ph.D. study.

6.1 Part A

Figure 6.1 shows an overview of the content of Part A. Dashed lines and italic text denotes ongoing work related to the methods and models presented in Part A. The three blocks are described here:

Publication 1: Journal paper regarding accounting for closely spaced modes when comparing finite element method mode shapes to experimental mode shapes. Written in collaboration with Martin Juul (1st author).

Publication 2: Investigation of Stewart-Gough platform performance for the InnoMill machine case. The platform is attached to the Vestas V112-3.0 MW hub at locations required to machine the entire part. Workspace-, singularity- and static force analysis is conducted. Rigid base results are compared to elastic base results.

New Model: Finite element based vibrational model of Stewart-Gough platform including elasticity of moveable platform and lateral stiffness of actuators is to be derived. Results will be compared to experimental results provided by Martin Juul. The purpose is to update parameters of the Stewart-Gough platform model such that the vibrational response of the model matches the vibrational response measured on the MOOG MB-E-6DOF/24/1800KG Motionbase at Aarhus University.

6.2 Part B

Aside from the future work based on Part A the main goal of Part B is illustrated in Figure 6.2. A parametric flexible multibody dynamics simulation framework will be designed using the Python interface of Adams multibody dynamics simulation software. Knowledge obtained in Part A regarding workpiece and machine will be utilised in development of the framework. The model requires a workpiece model, a machine model, G-code and a model of the machine-workpiece interface. Built-in Adams forward dynamics- and vibrational response solvers are used, and results are post processed in the *Tolerance Prediction Model*. Building realistic and computationally efficient multibody dynamic models of the linear actuators of the Stewart-Gough platform is expected to be challenging. An initial literature study on the subject will be conducted, and different simplified models will be investigated. In Adams flexibility is included using reduced order models (Craig Bampton Reduction) to increase computational efficiency. Continuous material removal is not possible in Craig Bampton reduced models, but based on the workpiece studies (Section 3.3) the vibrational response of the hub does not change considerably. Therefore, property changes of the hub are accounted for by precomputing reduced models for different stages of the process.

The *Tolerance Prediction Model* analyses whether the actual machined geometry is within tolerance requirements, and whether the process is stable using stability lobe diagrams. Thus the *Tolerance Prediction Model* can be utilised for process optimisation prior to the actual machining process.

Since the model is build in a parametric manner it is possible to investigate impact of uncertainties using the model. An example is investigation of maximum allowable error in positioning the machine anchor points on the workpiece. By introducing some random error to the interface points in the model, and running the model for several different random combinations it is possible to give recommendations regarding maximum allowable error in the real life setup.
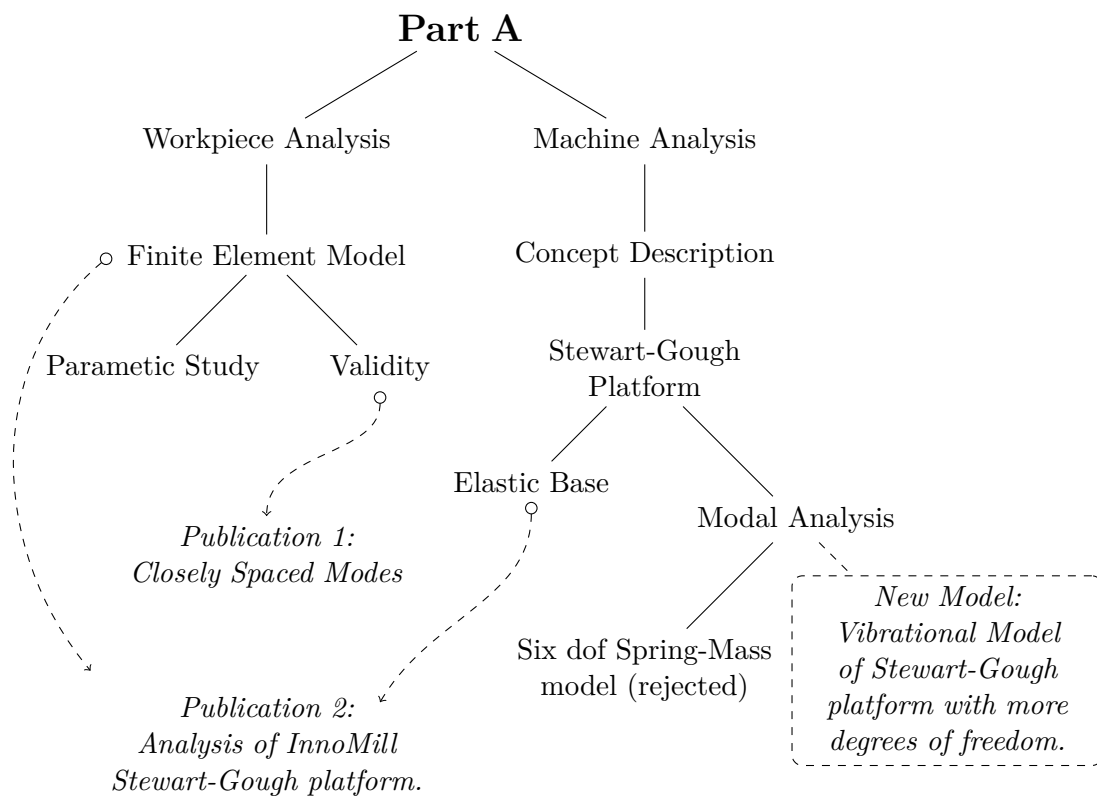
Figure 6.1: Overview of Part A content. Dashed lines illustrates future work related to Part A.

Part B

*Parametric Flexible
Multibody Dynamics
Simulation Framework
(Adams Python API)*

Workpiece Model   **Machine Model**   **G-Code**

Interface Model   G-Code Interpreter

Multibody Dy-   Actuator Motion
namics Model

Adams Solver
(Forward Dynamics and Vibrational Response)

Tolerance Prediction Model

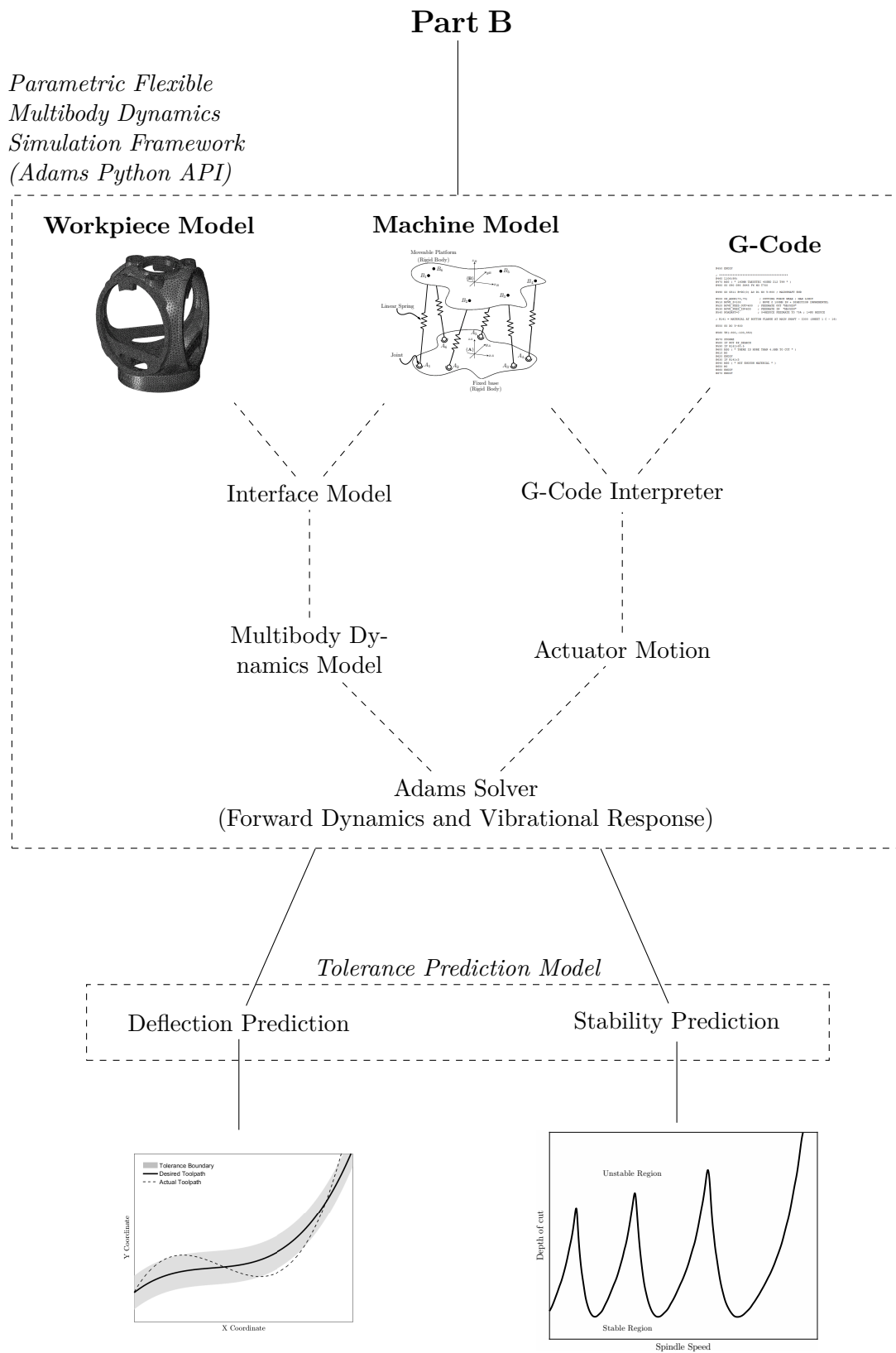Deflection Prediction   Stability Prediction

Figure 6.2: Overview of Part B content.

Bibliography

[1] L Uriarte, M Zatarain, D Axinte, J Yagüe-Fabra, S Ihlenfeldt, J Eguia, and A Olarra. Machine tools for large parts. *CIRP Annals-Manufacturing Technology*, 62(2):731–750, 2013.

[2] J Munoa, X Beudaert, Z Dombovari, Y Altintas, Erhan Budak, C Brecher, and G Stepan. Chatter suppression techniques in metal cutting. *CIRP Annals-Manufacturing Technology*, 65(2):785–808, 2016.

[3] U Bravo, O Altuzarra, LN López De Lacalle, JA Sánchez, and FJ Campa. Stability limits of milling considering the flexibility of the workpiece and the machine. *International Journal of Machine Tools and Manufacture*, 45(15):1669–1680, 2005.

[4] Svetan Ratchev, Stan Nikov, and Idir Moualek. Material removal simulation of peripheral milling of thin wall low-rigidity structures using fea. *Advances in Engineering Software*, 35 (8):481–491, 2004.

[5] R Ramesh, MA Mannan, and AN Poo. Error compensation in machine tools a review: part i: geometric, cutting-force induced and fixture-dependent errors. *International Journal of Machine Tools and Manufacture*, 40(9):1235–1256, 2000.

[6] H Schwenke, W Knapp, H Haitjema, A Weckenmann, R Schmitt, and F Delbressine. Geometric error measurement and compensation of machines an update. *CIRP Annals-Manufacturing Technology*, 57(2):660–675, 2008.

[7] A Olarra, D Axinte, L Uriarte, and R Bueno. Machining with the walkinghex: A walking parallel kinematic machine tool for in situ operations. *CIRP Annals-Manufacturing Technology*, 2017.

[8] Serope Kalpakjian, Steven R Schmid, and KS Vijay Sekar. *Manufacturing engineering and technology.* Pearson Upper Saddle River, NJ, USA, 2014.

[9] Robert D Cook et al. *Concepts and applications of finite element analysis.* John Wiley & Sons, 2007.

[10] Dassault Systemes Simulia Corporation. Abaqus 6.14. https://www.3ds.com/products-services/simulia/products/abaqus/, 2014.

[11] Kasper Ringgaard and Ole Balling. Modelling of material removal on large wind turbine hub. In *Proceedings of the 4th Joint Intl. Conference on Multibody System Dynamics*, 2016.

[12] Kasper Ringgaard and Alessandro Checchi. Milestone report 2.1, preliminary hub sensitivity analysis. Technical report, InnoMill Consortium, Aarhus University, 2016.

[13] Emese Kovacs. Operational modal analysis on a wind turbine hub. Master's thesis, Aarhus University, June 2016.

[14] Martin Juul, Emese Kovacs, Rune Brincker, and Ole Balling. Oma identification of a wind turbine rotor hub for monitoring purpose. In *Proceedings of the 2016 Leuven Conference on Noise and Vibration Engineering*, 2016.

[15] Randall J Allemang. The modal assurance criterion–twenty years of use and abuse. *Sound and vibration*, 37(8):14–23, 2003.

[16] Martin Juul, Kasper Ringgaard, Ole Balling, and Rune Brincker. Closely spaced modes in multi setup operational modal analysis. 2017.

[17] John J Craig. *Introduction to robotics: mechanics and control*, volume 3. Pearson Prentice Hall Upper Saddle River, 2005.

[18] Zoran Pandilov and Vladimir Dukovski. Comparison of the characteristics between serial and parallel robots. *Acta Technica Corviniensis-Bulletin of Engineering*, 7(1):143, 2014.

[19] Jean-Pierre Merlet. *Parallel robots*, volume 74. Springer Science & Business Media, 2012.

[20] Hamid D Taghirad. *Parallel robots: mechanics and control*. CRC press, 2013.

[21] YD Patel, PM George, et al. Parallel manipulators applications a survey. *Modern Mechanical Engineering*, 2(03):57, 2012.

[22] H Asada and J Granito. Kinematic and static characterization of wrist joints and their optimal design. In *Robotics and Automation. Proceedings. 1985 IEEE International Conference on*, volume 2, pages 244–250. IEEE, 1985.

[23] Clément M Gosselin and Eric Lavoie. On the kinematic design of spherical three-degree-of-freedom parallel manipulators. *The International Journal of Robotics Research*, 12(4): 394–402, 1993.

[24] Clément M Gosselin and J-F Hamel. The agile eye: a high-performance three-degree-of-freedom camera-orienting device. In *Robotics and Automation, 1994. Proceedings., 1994 IEEE International Conference on*, pages 781–786. IEEE, 1994.

[25] K-M Lee and Dharman K Shah. Kinematic analysis of a three-degrees-of-freedom in-parallel actuated manipulator. *IEEE Journal on Robotics and Automation*, 4(3):354–360, 1988.

[26] A Fattah and GH Kasaei. Kinematics and dynamics of a parallel manipulator with a new architecture. *Robotica*, 18(05):535–543, 2000.

[27] VE Gough. Contribution to discussion of papers on research in automobile stability, control and tyre performance. In *Proc. Auto Div. Inst. Mech. Eng*, volume 171, pages 392–394, 1956.

[28] Edward J Haug. *Computer aided kinematics and dynamics of mechanical systems*, volume 1. Allyn and Bacon Boston, 1989.

[29] Singiresu S Rao and Fook Fah Yap. *Mechanical vibrations*, volume 4. Prentice Hall Upper Saddle River, 2011.

Ringgaard, Kasper. Development of Mobile Machining Cell, 2017

Department of Engineering
Aarhus University
Inge Lehmanns Gade 10
8000 Aarhus N
Denmark